Characterization and Topology of the Membrane Domain Nqo10 Subunit of the Proton-Translocating NADH-Quinone Oxidoreductase of *Paracoccus denitrificans*†

Mou-Chieh Kao, Salvatore Di Bernardo, Akemi Matsuno-Yagi, and Takao Yagi*

Division of Biochemistry, Department of Molecular and Experimental Medicine, The Scripps Research Institute, 10550 North Torrey Pines Road, La Jolla, California 92037

Received January 30, 2003; Revised Manuscript Received March 3, 2003

ABSTRACT: The proton-translocating NADH-quinone oxidoreductase (NDH-1) of *Paracoccus denitrificans* is composed of 14 different subunits (Nqo1−Nqo14). Of these, seven subunits (Nqo7, Nqo8, and Nqo10−14) which are equivalent to the mitochondrial DNA-encoded subunits of complex I constitute the membrane segment of the enzyme complex; the remaining subunits make up the peripheral part of the enzyme. We report here on the biochemical characterization and heterologus expression of the Nqo10 subunit. The Nqo10 subunit could not be extracted from the *Paracoccus* membranes by NaI or alkaline treatment, which is consistent with the presumed membrane localization. By using the maltose-binding protein (MBP) fusion system, the Nqo10 subunit was overexpressed in *Escherichia coli*. The MBP-fused Nqo10 was expressed in membrane fractions of the host cell and was extractable by Triton X-100. The extracted fusion protein was then isolated by one-step affinity purification through an amylose column. By using immunochemical methods in conjunction with cysteine-scanning mutagenesis and chemical modification techniques, the topology of the Nqo10 subunit expressed in *E. coli* membranes was determined. The data indicate that the Nqo10 subunit consists of five transmembrane segments with the N- and C-terminal regions facing the periplasmic and cytoplasmic sides of the membrane, respectively. In addition, the data also suggest that the proposed topology of the MBP-fused Nqo10 subunit expressed in *E. coli* membranes is consistent with that of the Nqo10 subunit in the native *Paracoccus* membranes. From the experimentally determined topology together with computer prediction programs, a topological model for the Nqo10 subunit is proposed.

A Gram-negative soil bacterium *Paracoccus denitrificans* closely resembles the mammalian mitochondria when grown in aerobic conditions and possesses a mitochondrial-type respiratory chain (*1*). The proton-translocating NADH-quinone oxidoreductase of *Paracoccus* (NDH-1),[1] like the mammalian enzyme (complex I), is a multiple subunit enzyme complex that is responsible for electron transfer from NADH to quinone with the coupled translocation of protons across the membrane (*2*). Compared to mammalian complex I, which is composed of at least 46 different subunits (*3*) and recognized as the most intricate membrane-associated enzyme complex, the *Paracoccus* NDH-1 is relatively simpler with only 14 different subunits (designated Nqo1−14) (*4*, *5*). However, in terms of cofactors, the *Paracoccus* enzyme is similar to the mammalian enzyme and bears one noncovalently bound FMN and eight iron−sulfur clusters (*2*). Therefore, it provides a useful model system for studying the structure and function of the mitochondrial complex I.

Low resolution structures obtained from electron microscopic analyses of complex I/NDH-1 of *Neurospora crassa* (*6*), *E. coli* (*7*), and bovine mitochondria (*8*) indicate that this enzyme complex has an L-shaped assembly with one arm in the membrane and the other in the matrix or cytoplasm. Results based on membrane extraction studies suggest that the *Paracoccus* NDH-1 can also be divided into two segments, the peripheral domain and the membrane domain (*9*, *10*). The peripheral domain in the *Paracoccus* NDH-1 protrudes into the cytoplasm and is composed of seven subunits (Nqo1−6 and Nqo9 subunits) (*9*, *10*). It contains all the prosthetic groups involved in the NADH-quinone oxidoreductase reaction (*2*, *11*, *12*). Among these subunits, subunits Nqo1−5 appear to be solely in the peripheral part. The Nqo6 and Nqo9 subunits, on the other hand, have been experimentally demonstrated to be partly present in the membrane, and are believed to act as a connector between the peripheral segment and the membrane segment (*2*, *9*, *13*). In addition, cross-linking experiments

† This work was supported by United States Public Health Science Grant R01GM33712. Synthetic oligonucleotides and DNA sequencings were, in part, supported by the Sam & Rose Stein Endowment Fund. This is publication 15529-MEM from The Scripps Research Institute, La Jolla, CA.

* To whom correspondence should be addressed: Tel: (858) 784-8094. Fax: (858) 784-2054. E-mail: yagi@scripps.edu.

[1] AIAS, 4-acetamido-4′-[(iodoacetyl)amino]stilbene-2,2′-disulfonic acid; AEBSF, 4-(2-aminoethyl)benzenesulfonyl fluoride; complex I, mitochondrial proton-translocating NADH-quinone oxidoreductase; DTT, dithiothreitol; EDTA, ethylenediaminetetraacetic acid; EPR, electron paramagnetic resonance; FMN, flavin mononucleotide; GST, glutathione-*S*-transferase; IPTG, isopropyl *β*-D-thiogalactopyranoside; ISO, inside-side-out; MBP, maltose-binding protein; NDH-1, bacterial proton-translocating NADH-quinone oxidoreductase; NEM, *N*-ethylmaleimide; PBS, phosphate-buffered saline; PCR, polymerase chain reaction; PMSF, phenylmethanesulfonyl fluoride; Q, quinone; RSO, right-side-out; SMP, submitochondrial particles; SDS−PAGE, sodium dodecyl sulfate−polyacrylamide gel electrophoresis; TES buffer, 0.2 M Tris-HCl (pH 8.0) containing 5 mM EDTA and 0.5 M sucrose; TMA-DPH, 1-(4-trimethylammoniumphenyl)-6-phenyl-1,3,5-hexatriene.

10.1021/bi034166z CCC: $25.00
Published on Web 03/28/2003

Table 1: Oligonucleotide Primers Used for Site-Directed Mutagenesis in MBP-Fused *Paracoccus* Nqo10 Subunit

mutation	mutagenic primer sequence[a]	codon change
C14S	5′ GATCAGCGCCA*GCGTCGCCG 3′	TGC → AGC
M2C	5′ GGATCCCGAGGAATGT*G*C*ACCTTCGCTTTCTAC 3′	ATG → TGC
N25C	5′ GTGATCGGCCGCT*G*CCCGGTGCATTC 3′	AAC → TGC
A49C	5′ TCGTGCTGCAAGGCT*G*C*GAGTTCGTCGCCATG 3′	GCG → TGC
E50C	5′ TGCTGCAAGGCGCGT*G*C*TTCGTCGCCATGC 3′	GAG → TGC
G84c	5′ CCGAGCTGAAGT*GCGAACTGGCGC 3′	GGC → TGC
S114C	5′ GCTGGACGCCCTG*C*GACCAGGCCGAAAG 3′	TCG → TGC
R142C	5′ CGTGCTTTACGACT*GCTATGTGCTGATG 3′	CGC → TGC
H168C	5′ CTGACCATGCGCT*G*CCGCAAGGACGTC 3′	CAC → TGC
W182C	5′ GAACAGATGTGC*CGCGACCCGGC 3′	TGG → TGC

[a] Asterisks indicate mismatches.

provided clear evidence that the Nqo6 subunit directly interacts with the membrane domain Nqo7 subunit (*14*).

The membrane domain of the *Paracoccus* NDH-1 appears to consist of seven subunits (Nqo7, Nqo8, and Nqo10−14) (*15*, *16*), which are homologues of the mitochondrial DNA (mtDNA)-encoded subunits of mammalian complex I (*17*, *18*). Unlike the peripheral domain, no cofactor has been identified in this membrane-bound segment. Other than the primary structure deduced from nucleotide sequences, information on the membrane domain subunits is scarce. It is apparent that the membrane segment is involved in proton translocation and Q-binding (*2*, *19*). Because the structure and arrangement of the membrane domain subunits are crucial to an understanding of the mechanism of proton translocation, we have undertaken detailed studies on the properties and characteristics of the individual subunits in the membrane segment (*2*, *20*, *21*).

In this paper, we focused on the *Paracoccus* Nqo10 subunit (a counterpart of the ND6 subunit of complex I). Recently, it has been recognized that the ND6 gene of complex I is a hot spot for pathogenic mutations (*22*), and numerous point mutations leading to amino acid changes in this subunit have been found to be associated with known mitochondrial diseases. We were able to overexpress the *Paracoccus* Nqo10 subunit in membrane fractions of *E. coli* by using the MBP fusion system. Characterization and the topological studies of the Nqo10 subunit were carried out and a possible relevance of the structure of this subunit to mitochondrial diseases is discussed.

EXPERIMENTAL PROCEDURES

Antibody Production. An oligopeptide, H-CELKDVK-PGQGL-OH (Nqo10c), derived from the C-terminal region of the *Paracoccus* Nqo10 subunit with an additional cysteine incorporated for the purpose of conjugation was linked to maleimide-activated bovine serum albumin as an immunogen using Imject Activated Immunogen Conjugation kit. Antibodies were raised in rabbits and were affinity-purified according to published procedures (*23*−*25*).

Construction of the MBP-Fused Nqo10 Expression Vector. The *nqo10* gene used for expression and mutagenesis was constructed from pXT-2b plasmid (*16*) utilizing PCR. Two oligonucleotides, 5′-TCTATGCCGAGGATCCCGAGGAAT-GATG-3′ and 5′-CTATCGCGGTCAAGCTTGCCGCGTTC-3′, were synthesized in which the underlined bases were altered from *Paracoccus* DNA to generate a *Bam*HI site and a *Hin*dIII site near the initiation and stop codon, respectively, of the *nqo10* gene. By using pXT-2b plasmid as a template and the designed oligonucleotides as primers, PCR amplification of the *nqo10* gene was carried out in a thermocycler as described previously (*26*). The amplified DNA was subcloned into pCR-Script Amp SK(+), and its sequence was confirmed by sequencing. The resulting plasmid was designated pCR(Nqo10). The pCR(Nqo10) was digested with *Bam*HI/*Hin*dIII, and the DNA fragment containing the desired *nqo10* gene was then purified and ligated in the *Bam*HI/*Hin*dIII sites of the pMAL-p2G vector. The plasmid thus obtained was named pMAL-p2G(Nqo10), which is a fusion plasmid with the inserted *nqo10* gene located immediately downstream from and in the same translational reading frame as the vector's *malE* gene.

Mutagenesis and Production of Monocysteine Derivatives of nqo10. Mutants for cysteine-scanning experiments were constructed by using the GeneEditor in vitro site-directed mutagenesis system (Promega) according to the manufacturer's instructions. First, a plasmid, named pCR(Nqo10)-(C14S), was constructed in which the sole endogenous cysteine (Cys14) existing in Nqo10 was replaced with serine to produce a cysteine-less mutant. By using this cysteine-less background, a synthetic oligonucleotide listed in Table 1, which contained the desired codon change, could replace a specific amino acid residue with a cysteine. All mutated *nqo10* genes were verified by DNA sequencing before being subcloned into the pMAL-p2G vector to allow expression of the MBP-fused protein in the host cells for cysteine labeling experiments.

Expression of the MBP-Fused Nqo10 Subunit. Competent *E. coli* BLR(DE3)pLysS cells were transformed with derivatives of plasmid pMAL-p2G carrying wild-type *nqo10*, cysteine-less *nqo10*, or various *nqo10* mutations and spread onto LB agar plate containing 100 μg/mL ampicillin. Cells were grown at 37 °C basically as reported previously (*21*) except that IPTG was added at 0.5 mM when the culture reached A_{600} of ∼2.0. The cells were then harvested by centrifugation and stored at −80 °C, or immediately used for preparation of membrane vesicles.

Purification of the MBP-Fused Nqo10 Subunit. The cell pellet was suspended (1 g of cells/10 mL) in 20 mM Tris-HCl (pH 8.0) containing 1 mM EDTA, 1 mM DTT, 0.3 M NaCl, and 1 mM PMSF (buffer A). The cell suspension was freeze-thawed twice, sonicated briefly before passing through a French press at 1500 psi to thoroughly disrupt the cells. After cell debris and insoluble materials were removed by repeated centrifugations in a Sorvall SS34 rotor at 12 000 rpm for 10 min, the resulting cell lysate was ultracentrifuged at 50 000 rpm for 30 min in a Beckman Spinco 60Ti rotor

to separate soluble (cytosol) and membrane fractions. The collected membrane fractions were resuspended to 5 mg/mL protein in buffer A containing 1% (v/v) Triton X-100. The suspension was placed in an ice−water bath and sonicated with a Branson sonifier attached to a narrow tip at an amplitude of 6 with 50% pulse for 5 min 3 times. Following sonication, the sample was incubated on ice for 1 h and then subjected to ultracentrifugation at 50 000 rpm for 1 h in a 60Ti rotor. The supernatant fraction was collected and loaded onto an amylose column (5 mL of bed volume) equilibrated with buffer A plus 0.5% Triton X-100 (column buffer). After washing with 20 column volumes of the column buffer, the MBP-fused *Paracoccus* Nqo10 was eluted from the column with 10 mM maltose, concentrated in an Amicon Centriprep-30 concentrator, and stored at −20 °C.

The pMAL-p2G vector includes a sequence coding for the recognition site (PGAAHY) of Genenase I. To separate the Nqo10 protein from MBP, the purified MBP-fused *Paracoccus* Nqo10 subunit was first adjusted to 0.5 mg/mL in buffer A and then digested with Genenase I at 0.01 mg/mL at room temperature for 24 h.

Preparation of ISO and RSO Membrane Vesicles of Paracoccus and E. coli. ISO membrane vesicles were prepared as described previously (*20*, *21*) with some minor modifications. Briefly, the cells were suspended at ∼40 mg/mL (wet weight) in a buffer containing 50 mM Tris-HCl, pH 7.5, 5 mM $MgCl_2$, 1 mM DTT, and 1 mM PMSF. The cell suspension was then passed through a French press once at 8000 psi. After unbroken cells and large cell debris were removed by repeated centrifugations at 12 000 rpm for 10 min in a SS34 rotor, ISO membrane vesicles were collected from the supernatant by centrifugation at 50 000 rpm for 30 min in a 60Ti rotor. The resulting pellet was resuspended in 50 mM Tris-HCl (pH 7.5) containing 5 mM $MgCl_2$, 1 mM PMSF, and 0.5 M sucrose. RSO membrane vesicles were prepared according to an established method based on lysozyme-EDTA treatment and osmotic lysis (*27*, *28*). The concentration of the total membrane proteins in ISO and RSO membrane vesicles was determined by the BCA protein assay kit (Pierce) according to manufacturer's protocol after solubilization of the membranes in 2% SDS.

Chemical Labeling and Blocking. ISO and RSO membranes vesicles were collected by centrifugation, washed once with labeling buffer (50 mM Tris-HCl (pH 7.5), 5 mM $MgCl_2$, 1 mM PMSF, and 0.5 M sucrose), and resuspended in the same buffer to give a final protein concentration of 17 mg/mL. Approximately 5 mg of membrane protein was used for the labeling reaction. Eight microliters of the freshly prepared blocking reagent, AIAS (40 mM), or the same volume of distilled water was added to the membrane vesicles, followed by incubation at room temperature for 2 h in the dark. Subsequently, the reaction mixture was treated with 3 μL of 1 mCi/mL [^{3}H]NEM and incubated at room temperature for 2 h. The reactions were quenched with 50 mM cysteine and incubation for 30 min. A stock solution of 1 M cysteine was prepared just prior to use in labeling buffer. After quenching, the membrane vesicles were disrupted by freeze−thawing twice, followed by the addition of Triton X-100 in buffer A to a final concentration of 3% and incubation for 2 h to solubilize the membranes. The Triton X-100 extract was then recovered from centrifugation and mixed with 120 μL of amylose resin (preequilibrated with buffer A). After overnight incubation at 4 °C, the resin was washed repeatedly with 1 mL of buffer A for 4 times. The MBP−Nqo10 was then eluted with 10 mM maltose in 100 μL of elution buffer (80 mM Tris-HCl, pH 6.8, 6% SDS, and 20% glycerol) for 2 h at room temperature. Each collected sample was mixed with 5 mL of scintillation cocktail and radioactivity was measured in the Beckman LS-6000SC Liquid Scintillation System.

Preparation of Liposomes and Reconstitution of the MBP-Fused Nqo10 Subunit. Detailed procedures for liposome preparation and fusion protein reconstitution have been described previously (*20*, *21*). Briefly, liposomes were first prepared by mixing a chloroform/methanol (2:1) solution of phosphatidylcholine (type XVI-E) with 1-(4-trimethylammoniumphenyl)-6-phenyl-1,3,5-hexatriene (TMA-DPH) in a molar ratio 200:1. The solvent was evaporated under argon flux, and the lipid film was then hydrated in 10 mM Tris-HCl (pH 8.0) to a phospholipid concentration of 10 mg/mL with agitation. The resultant suspension was sonicated on ice 8 times with 50% pulse mode for 5 min each, followed by the addition of dodecyl maltoside until its turbidity disappeared (approximately 2.25 mol of detergent/mol of phospholipid). During the reconstitution process aliquots of the purified MBP-fused Nqo10 subunit were added to the equilibrated detergent-phospholipid suspension to give the protein-to-lipid ratios of 0, 5, 10, 25, and 50% (w/w), and the resultant mixture was incubated at room temperature for 1 h. To remove the detergent, the suspension was mixed with SM2 Bio-Beads (10 mg/mg of phospholipid) according to the batch procedure originally described by Holloway (*29*), and incubated at room temperature with gently agitation for 2 h. The SM2 beads were then removed by centrifugation. The collected liposome suspension was dialyzed against 10 mM Tris-HCl (pH 8.0) overnight with a Pierce Slide-A-Lyzer 10k Dialysis Cassette. The fluorescence anisotropy of the reconstituted MBP-fused Nqo10 liposomes were carried out at 25 °C according to refs *30* and *31* in an SLM 8000 spectrofluorometer. The excitation and emission wavelengths were 363 and 429 nm, respectively. For control experiments, the MBP-fused Nqo10 subunit was replaced by MBP2*, which is a derived, soluble protein that consists of maltose-binding protein preceded by methionine and with the final four amino acids replaced by 23 extra amino acid residues.

Sequence Analysis. The GCG software package was used to analyze the DNA and amino acid sequences (*32*). The BESTFIT, PILEUP, and PRETTYBOX programs were used to conduct the sequence alignment and comparison. Homology search was carried out using the BLAST server at the National Center for Biotechnology Information (*33*). Topological prediction of membrane proteins was performed on web servers for TMHMM (*34*), HMMTOP (*35*), MEMSAT (*36*), TopPred2 (*37*), TMpred (*38*), and PHD (*39*). All prediction methods were used in their single-sequence mode with all user-adjustable parameters left at their default values.

Other Analytical Procedures. Protein concentration was determined by the BCA protein assay kit (Pierce) according to the manufacturer's protocol. SDS−PAGE was performed using the discontinuous system of Laemmli (*40*). Instead of boiling, protein samples were incubated at room temperature for 1 h before being loaded onto the gel. Immunoprecipitation with anti-Nqo10c serum was conducted according to a protocol previously described (*41*, *42*). Any variations from

the procedures and other details are described in the figure legends.

Materials. The pCR-Script Amp Cloning kit was from Stratagene (La Jolla, CA). The GeneEditor in vitro Site-Directed Mutagenesis system was purchased from Promega (Madison, WI). Materials for PCR product purification, plasmid preparation, and gel extraction were obtained from Qiagen (Valencia, CA). Amylose resin, anti-MBP antiserum, MBP2*, expression vector pMAL-p2G, and Genenase I were from New England Biolabs (Beverly, MA). Protein A Sepharose CL-4B gel was purchased from Amersham Pharmacia Biotech (Arlington Heights, IL). SM2 Bio-Beads were from Bio-Rad (Hercules, CA). IPTG and PMSF were from Sigma (St. Louis, MO). BCA protein assay kit, GelCode Blue stain reagent, SuperSignal West Pico chemiluminescent substrate, and Imject Activated Immunogen Conjugation kit were from Pierce (Rockford, IL). *N*-Ethyl-[1,2-^{3}H]maleimide was from NEN (Boston, MA). 4-Acetamido-4′-[(iodoacetyl)-amino]stilbene-2,2′-disulfonic acid sodium salt was from Molecular Probes (Eugene, OR). All other materials were reagent grade and obtained from commercial sources.

RESULTS

Production of Antibodies against the Paracoccus Nqo10 Subunit. Because of their hydrophobic nature, membrane subunits in complex I are difficult to purify and usually provide limited immunogenicity. However, peptide antibodies have been successfully raised against some of the membrane domain subunits in human complex I (*17*, *43*) as well as in *Paracoccus* NDH-1 (*20*, *21*). Thus, we attempted to raise antibodies to the *Paracoccus* Nqo10 subunit using synthetic oligopeptides corresponding to the C- or N-terminal regions. Unfortunately, oligopeptides derived from the N-terminal region were too hydrophobic to synthesize and purify. In contrast, antibody against the C-terminal 11 amino acid residues of the Nqo10 subunit (designated anti-Nqo10c) was successfully produced. The antibody, when tested against the *Paracoccus* membranes, clearly recognized a single band of a M_r ~21 kDa, which coincides with the MW = 21 947 of the Nqo10 subunit deduced from its amino acid sequence (Figure 1A). The anti-*Paracoccus*-Nqo10c antibody also recognized a band with a similar M*r* in the *Rhodobacter capsulatus* membranes (The Nqo10 homologue has a MW = 21 733 calculated from the deduced amino acid sequence). The same antibody did not react with *Thermus thermophilus* HB-8 membranes, *E. coli* membranes, or bovine heart SMP. These results are not unexpected because the selected C-terminal region of the *Paracoccus* Nqo10 subunit exhibits 82% sequence identity to the Nqo10 homologue of *R. capsulatus* but are significantly different in other organisms tested (Figure 1A). Furthermore, the anti-Nqo10c antibody was able to immunoprecipitate a protein with the same mass from the cholate-treated *Paracoccus* membranes (Figure 1B).

Localization of the Nqo10 Subunit in the Paracoccus NDH-1. Our previous experiments demonstrated that the peripheral subunits of the *Paracoccus* NDH-1 (Nqo1−6 and 9) can be extracted from the membranes by a chaotropic agent such as NaI or by incubation at high pH, whereas the membrane subunits Nqo7 and Nqo11 remain in the membrane after these treatments (*9*, *10*, *21*). With the antibody to the Nqo10 subunit available, we were able to conduct the same extraction experiments for this subunit. As seen in Figure 2, the peripheral subunit Nqo1 (the NADH-binding subunit) was partially extracted from the membranes by

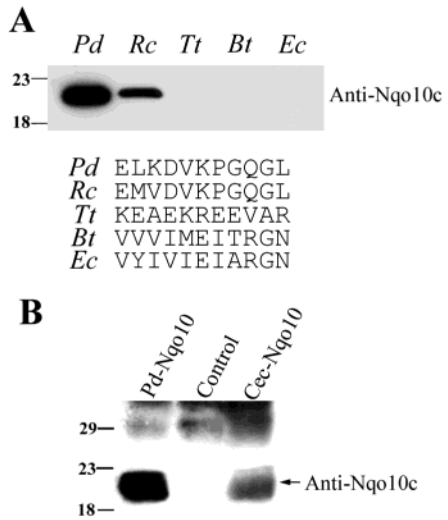

FIGURE 1: Reactivity of anti-*Paracoccus* Nqo10c antibody. The antibody was raised against the C-terminal 11 amino acids of the *Paracoccus* Nqo10 subunit and affinity-purified as detailed in the Experimental Procedures. (A) Cross-immunoreactivity with the *Paracoccus* membranes (*Pd*), *R. capsulatus* chromatophores (*Rc*), *T. thermophilus* HB-8 membranes (*Tt*), bovine heart SMP (*Bt*), and *E. coli* membranes (*Ec*). Gel electrophoresis and electronic transfer were carried out using 10 μg each of the samples as described previously (*23*−*25*). Immunoblotting was performed with the SuperSignal West Pico system (Pierce). The C-terminal amino acid sequences from the species are given for comparison. (B) Immunoprecipitation of the Nqo10 subunit from the *Paracoccus* membranes (Pd−Nqo10) and from Genenase I-treated, purified MBP-fused Nqo10 (Cec-Nqo10) by using anti-Nqo10c serum. In the control sample, *Paracoccus* membranes were treated with preimmune serum instead of anti-Nqo10c serum. The secondary antibody used for detection was goat anti-rabbit IgG, Fc fragment specific, horseradish peroxidase conjugate (Pierce). The numbers on the left side indicate the molecular mass (kDa) of marker proteins.

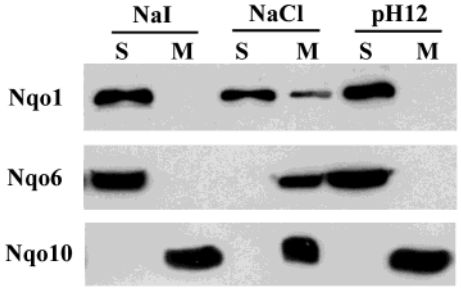

FIGURE 2: Effects of chaotropic reagents and alkaline buffer on extraction of the Nqo1, Nqo6, and Nqo10 subunits from cholate-treated *P. denitrificans* membranes. One hundred and twenty microliters of cholate-treated membranes (1.0 mg/mL) were incubated for 10 min at 30 °C either in the presence of 1.5 M NaI or 2.0 M NaCl (chaotrope treatment) or in a buffer, pH 12, containing 100 mM 2-(*N*-cyclohexylamino)-ethanesulfonic acid (alkaline treatment). The membrane suspension was then freeze-thawed twice using liquid nitrogen and a water bath at 30 °C followed by centrifugation in an Airfuge at 30 psi for 10 min. Ninety microliters of the supernatant was carefully transferred into microtubes. The resulting supernatant (S) and membrane suspensions (M) were mixed with equal volumes of 2× Laemmli's sample buffer. Ten microliters of each sample was loaded on Laemmli SDS-13% polyacrylamide gels. Immunoblotting was carried out with affinity-purified antibodies against Nqo1, Nqo6, and Nqo10c as described in Figure 1.

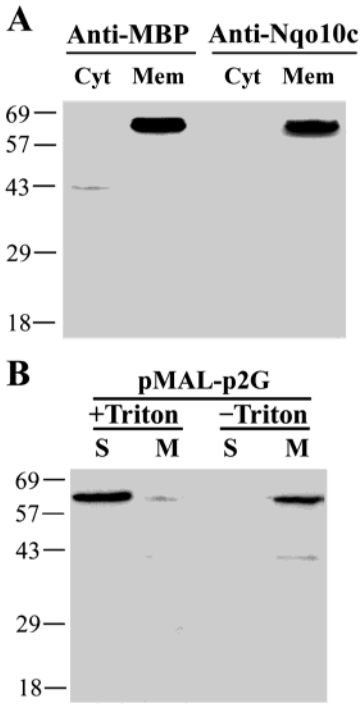

FIGURE 3: Expression of the MBP-fused Nqo10 subunit in *E. coli* membranes. The *Paracoccus* Nqo10 subunit was expressed in *E. coli* using the secretable MBP fusion system (pMAL-p2G). (A) Immunoblotting of the membrane fraction (Mem) and the cytosolic fraction (Cyt) prepared from the host *E. coli* cells bearing the pMAL-p2G(Nqo10) expression vector. Left panel, anti-MBP serum; right panel, affinity-purified anti-Nqo10c antibody. Ten micrograms of protein samples were applied to each lane of a 13% Laemmli gel. The electrophoresis and electronic transfer were carried out as described in Figure 1. (B) Triton extraction of the MBP-fused Nqo10 subunit from *E. coli* membranes. The membrane fraction (3.0 mg/mL) prepared from host cells was incubated in the presence or absence of 5% Triton X-100 for 1 h on ice. The supernatant (S) and the membrane suspensions (M) were prepared as given in Figure 2 and the samples were subjected to SDS−PAGE (13% polyacrylamide gel). Immunoblotting was conducted with affinity-purified anti-Nqo10c antibody. The numbers on the left side indicate the molecular mass (kDa) of marker proteins.

NaCl, but completely removed by NaI or at pH12. Similarly, another peripheral subunit Nqo6 (the connector subunit) could be extracted from the membranes except that this subunit resisted the NaCl treatment. In contrast, the Nqo10 subunit remained in the membranes under any conditions used. These data further confirmed that the Nqo10 subunit is one of the intrinsic hydrophobic proteins that make up the membrane segment of the *Paracoccus* NDH-1.

Expression of the Nqo10 Subunit in E. coli. For further characterization of the *Paracoccus* Nqo10 subunit, we attempted overexpression of this protein in a native form in *E. coli* membranes. For this purpose, we employed the secretable maltose-binding protein (MBP) fusion system. The MBP system has been successfully used for heterologous expression of foreign proteins in the bacterial system which would otherwise be difficult (*21*). Another advantage is that the MBP moiety attached to the N-terminus of a target protein provides useful information about the orientation of this end of the protein (*44*, *45*). As shown in Figure 3A, the MBP-fused Nqo10 subunit was expressed in membrane fractions of the host *E. coli* cell. Furthermore, the expressed protein could be extracted almost completely from the membrane fractions with 5% Triton X-100, indicating that

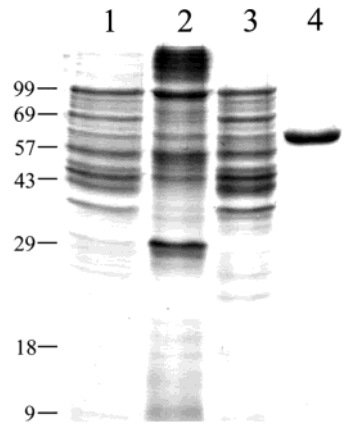

FIGURE 4: SDS−PAGE gel patterns of the MBP-fused *Paracoccus* Nqo10 subunit expressed in *E. coli*. Lane 1, cell lysate of *E. coli* expressing the MBP-fused *Paracoccus* Nqo10 subunit; lane 2, membrane fraction; lane 3, soluble fraction (cytoplasm); lane 4, MBP-fused Nqo10 subunit isolated by amylose affinity column chromatography. Ten micrograms (lanes 1−3) or 5 μg (lane 4) of sample proteins were loaded on a 13% Laemmli SDS gel. The protein was visualized with GelCode blue. The numbers on the left side indicate the molecular mass (kDa) of marker proteins.

the MBP-fused Nqo10 subunit may possess a correct folding in the membranes of the host cell (Figure 3B). In contrast, when the nonsecretable MBP system was used, the fusion protein was also located in the membrane fractions but was not extractable with Triton X-100 (data not shown). The MBP-fused Nqo10 subunit was then purified from the Triton X-100 extract to homogeneity by a one-step procedure using amylose affinity chromatography (Figure 4). The molecular weight estimated from SDS−PAGE of the MBP-fused Nqo10 subunit was 63.0 kDa, which agreed reasonably with the molecular size of the fusion protein (64.6 kDa) deduced from its amino acid sequence.

The purified MBP-fused Nqo10 subunit was then treated with Genenase I which cleaves the MBP protein. The cleavage of the MBP-fused Nqo10 subunit was partial. None of the attempts to improve the cleavage efficiency, including changing buffers and salt conditions, increasing reaction temperature, adding detergents, prolonging incubation and/or increasing Genenase I concentrations, was successful. It might be that three-dimensional conformation of the fusion protein hinders the accessibility of Genenase I to the cleavage site. As seen in Figure 5, the Genenase I treatment released two new cleavage products with molecular weights corresponding to 21 and 42 kDa. The molecular size and the immunoblotting results clearly identified the 21 kDa and the 42 kDa bands to be the Nqo10 subunit and the MBP, respectively. It should be noted that the 21 kDa band appeared diffuse and was poorly stained with the GelCode blue stain, which is indicative of a hydrophobic protein. In addition, the Genenase I-treated, MBP-fused Nqo10 subunit could be immunoprecipitated using the anti-Nqo10c antibody, further confirming the identity of the Nqo10 subunit (Figure 1B, right lane). These results suggest that the MBP-fused *Paracoccus* Nqo10 subunit was correctly expressed in the *E. coli* membranes.

It is expected that the MBP-fused Nqo10 subunit consists of a soluble, globular MBP domain and a hydrophobic, membrane-embedded Nqo10 domain. To confirm this point, we measured the effect of the MBP-fused Nqo10 subunit

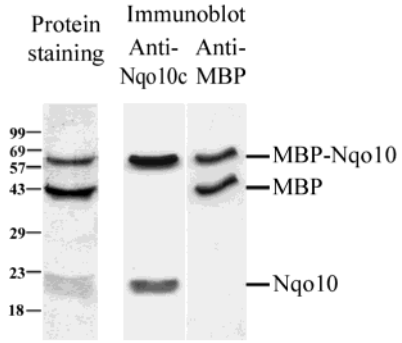

FIGURE 5: Identification of the cleaved fragments derived from the Genenase I-treated MBP-fused Nqo10 subunit by use of anti-Nqo10c antibody and anti-MBP serum. The purified MBP-fused Nqo10 protein was digested with Genenase I at room temperature for 24 h and the products were analyzed by electrophoresis and immunoblotting as described in Figure 1. Left panel, SDS gel pattern with GelCode blue staining; center panel, immunoblotting with affinity-purified anti-Nqo10c antibody; right panel, immunoblotting with anti-MBP serum. Ten micrograms (protein staining) and 2.5 μg (immunoblotting) of the sample protein were loaded per lane.

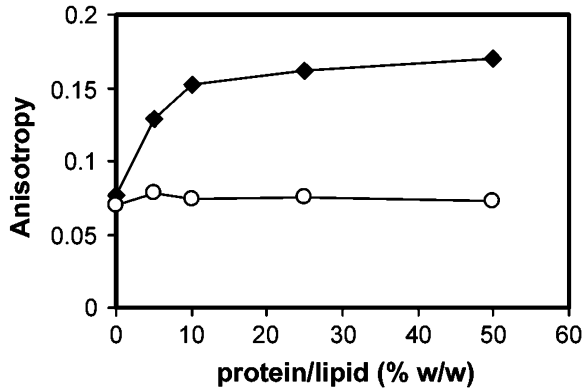

FIGURE 6: Effect of the MBP-fused *Paracoccus* Nqo10 subunit on the fluorescence anisotropy of phospholipid vesicles. The reconstituted phospholipid vesicles contained either MBP-fused *Paracoccus* Nqo10 subunit (◆) or MBP2* (○). Fluorescence anisotropy of TMA-DPH intercalated into the phospholipid vesicles was measured in a spectrofluorometer with the excitation and emission wavelengths at 363 and 429 nm, respectively.

on the fluorescence anisotropy of TMA-DPH in phospholipid vesicles. It is shown in Figure 6 that the anisotropy was increased by elevating the protein-to-lipid ratio. In contrast, the water-soluble protein MBP2* had no effects on the anisotropy. These results imply that the hydrophobic Nqo10 domain of the MBP-fused Nqo10 subunit interacted with the phospholipid vesicles and altered the microenvironment of TMA-DPH in the membrane. It is therefore likely that the MBP domain and the Nqo10 domain of the MBP-fused Nqo10 subunit behave independently.

Topological Studies of the Nqo10 Subunit. To carry out topological studies, the inside-out (ISO) and the right-side-out (RSO) membrane vesicles were prepared from *Paracoccus* and the host cell *E. coli* BLR(DE3)pLysS according to the methods outlined in Experimental Procedures. On the basis of our previous findings (*20*, *21*), the Nqo1 (NADH-binding) subunit and the C-terminal region of the Nqo7 subunit (Nqo7c) of the *Paracoccus* NDH-1 were selected as markers for the cytoplasmic and periplasmic sides of the membranes, respectively. The results of immuno-dot-blottng using the *Paracoccus* membranes indicate that the anti-Nqo1

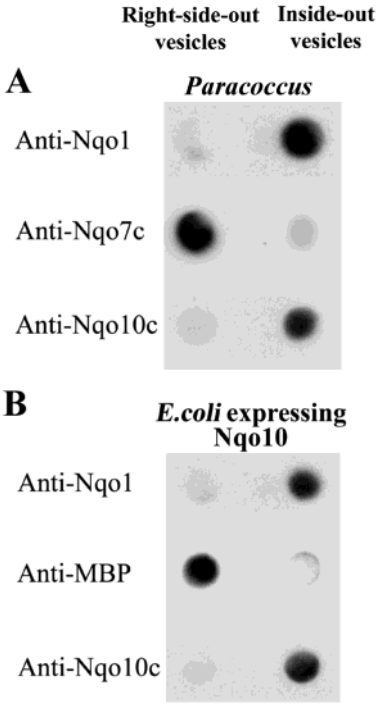

FIGURE 7: Localization of the C-terminal region of the Nqo10 subunit using oppositely oriented membrane vesicles. The right-side-out (RSO) and the inside-out (ISO) membrane vesicles were prepared from *Paracoccus* and *E. coli* cells as detailed in the Experimental Procedures. The membrane vesicles were bound directly to nitrocellulose membranes in a DOT Blot apparatus for 1 h at room temperature. After washing 3 times with TES buffer and incubation with 2% skim milk in PBS buffer for 1 h to block nonspecific binding sites, the nitrocellulose membranes were again thoroughly washed and incubated with the affinity-purified primary antibodies followed by detecting antibodies as described previously (*9*, *10*). The primary antibodies employed included antibodies directed against the Nqo1 protein and its *E. coli* homologue (positive control for ISO membrane vesicles), the Nqo7c protein (positive control for RSO membrane vesicles), the Nqo10 protein, and MBP. (A) *Paracoccus* membranes. (B) *E. coli* membranes expressing the MBP-fused Nqo10 subunit.

antibody recognized the ISO vesicles but did not recognize the RSO vesicles (Figure 7A). In contrast, the anti-Nqo7c antibody reacted with the RSO, but not ISO, membrane vesicles. These results confirm that the *Paracoccus* membrane vesicles were correctly prepared in terms of sidedness and reasonably low in contamination by the vesicles of opposite orientation. As seen in Figure 7A, the anti-Nqo10c antibody reacted with the ISO membrane vesicles but not with the RSO membrane vesicles, suggesting that the C-terminus of the Nqo10 subunit is exposed to the cytoplasmic side of the native *Paracoccus* membranes.

Using the same approach, we then examined the topology of the MBP-fused Nqo10 subunit expressed in the membranes of *E. coli* cells. As shown in Figure 7B, the antibody to the *E. coli* homologue of the Nqo1 subunit reacted with the ISO, but not RSO, *E. coli* membrane vesicles, which ensures the correct orientation and the quality of the prepared membrane vesicles. Antibody against MBP recognized the RSO, but not ISO, vesicles, confirming that the MBP domain of the fusion protein is present on the periplasmic side of the *E. coli* membranes. In contrast, the anti-Nqo10c antibody reacted with the ISO vesicles but not with the RSO vesicles. This result indicates that the C-terminus of the expressed

Table 2: Effect of the Membrane-Impermeable SH Modifier AIAS on [^{3}H]NEM-Labeling in the MBP-Fused *Paracoccus* Nqo10 Mutants

	right-side-out vesicle			inside-out vesicle			
mutation	+ AIAS (cpm)[a]	− AIAS (cpm)[a]	R[b]	+ AIAS (cpm)[a]	− AIAS (cpm)[a]	R[b]	location[c]
C14S (Cys-less)	270	362	1.3	298	369	1.2	−
M2C	451	971	2.2	438	631	1.4	P
N25C	297	391	1.3	468	1369	2.9	C
A49C	869	1266	1.5	723	1185	1.6	−
E50C	799	1319	1.7	822	1174	1.4	−
G84C	227	328	1.4	342	856	2.5	C
S114C	620	1494	2.4	854	983	1.2	P
R142C	1078	2931	2.7	689	1250	1.8	P
H168C	299	419	1.4	225	698	3.1	C
W182C	361	642	1.8	315	1603	5.1	C

[a] Values are the labeling collected from ^{3}H radioactivity counting. [b] *R* values are calculated by dividing the ^{3}H radioactivity counting from the samples without AIAS preincubation by the corresponding value from the samples with AIAS preincubation. [c] P, periplasm; C, cytoplasm; −, no location assigned.

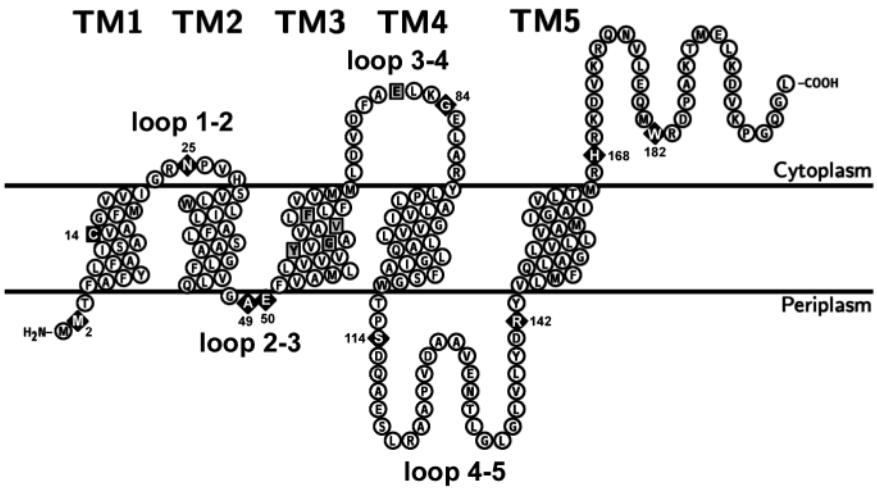

FIGURE 8: Proposed membrane topology of the *Paracoccus* Nqo10 subunit. Five putative transmembrane segments of the *Paracoccus* Nqo10 subunit from the N-terminus to the C-terminus are numbered with ascending Arabic numerals. The N-terminus and C-terminus are exposed to the periplasmic and cytoplasmic side of the membrane, respectively. The cysteine-less mutation is indicated by a black square. Residues replaced by a cysteine are shown as black diamonds with numbers representing the positions. Conserved residues among the homologues of the *Paracoccus* Nqo10 subunit are shown in gray squares. The topology plot presented here was generated by using the T_EXtopo package (*52*).

MBP-fused Nqo10 subunit faces the cytoplasm of the host *E. coli* cells. The concordance of the location of the C-terminus of the Nqo10 subunit in the *Paracoccus* membranes and that of the MBP-fused Nqo10 subunit in the *E. coli* membranes strongly suggests that the Nqo10 protein expressed in *E. coli* retains the native orientation.

Taking advantage of the possibility to generate mutants, we next examined the topology of membrane spanning segments of the MBP-fused Nqo10 subunit in the *E. coli* membranes using the substituted cysteine scanning analyses. Because the *Paracoccus* Nqo10 subunit contains one endogenous cysteine (Cys14), this residue was first replaced with a serine to prevent its possible interference. Because MBP has no naturally occurring cysteine, the cysteine-less MBP-fused Nqo10 subunit could be used directly to generate a series of Nqo10 subunit mutants, in each of which a single unique cysteine was introduced. On the basis of hydropathy plots of the *Paracoccus* Nqo10 subunit (see below), we selected nine cysteine residues in the positions corresponding to potential loops as well as the N- and the C-termini. The nine Nqo10 monocysteine mutants, M2C, N25C, A49C, E50C, G84C, S114C, R142C, H168C, and W182C, were generated and expressed in *E. coli*. All *E. coli* cells expressing the mutant proteins grew normally. The expression level and the subcellular distribution of each mutated MBP-fused Nqo10 subunit showed no substantial difference from those of the wide type.

The surface accessibility of the cysteine residue was assessed using the ISO and RSO *E. coli* membrane vesicles prepared from the host cells expressing the individual mutated Nqo10 subunits. These membrane vesicles were first incubated in the presence or absence of a membrane impermeable sulfhydryl reagent, AIAS, and then reacted with a membrane-permeable [^{3}H]NEM. The radiolabeled MBP-fused Nqo10 subunit was affinity-purified from the membranes using amylose resin and was subjected to radioactive analyses. Because MBP itself has no intrinsic cysteine, all radioactivity is presumed to derive from the labeling of the mutated Nqo10 subunit. The results of the radiolabeling experiments are summarized in Table 2. To assess the accessibility of the introduced cysteine residues, we calculated the ratio between the samples that were not treated with AIAS and those that were treated with AIAS. The values for the cysteine-less MBP-fused Nqo10 subunit were used as control for both the ISO and RSO vesicles. For example, in mutant M2C, the ratio obtained for the RSO vesicles was

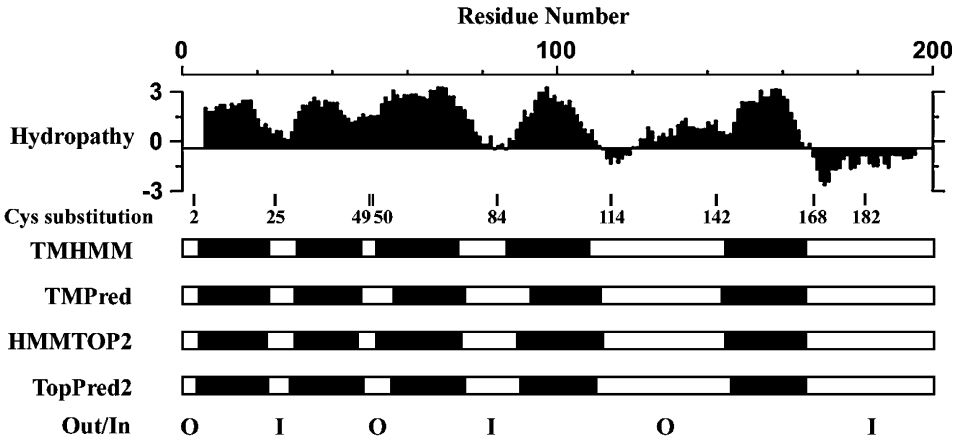

FIGURE 9: Topological characterization of the *Paracoccus* Nqo10 subunit based on predictions offered by a variety of computer programs. The hydropathy profile was obtained according to Kyte and Doolittle (*53*). Topological prediction was performed using web servers for TMHMM (*34*), TMpred (*38*), HMMTOP2 (*35*), and TopPred2 (*37*). All algorithms predicted five membrane spanning sections with the N-terminus on the outside (O) and the C-terminus on the inside (I). The residues replaced with a cysteine in this study are marked with bars and the residue numbers.

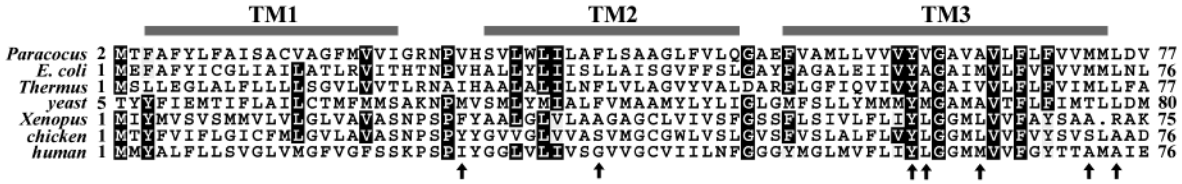

FIGURE 10: Comparison of the deduced primary sequence of the *Paracoccus* Nqo10 subunit with its homologues from various organisms. The region containing the first three membrane segments (TM1, TM2, and TM3) predicted in our model are shown. The alignment was conducted with the PILEUP program and conserved residues were highlighted with the PRETTYBOX program of the GCG package (*32*). The amino acid residues reported for pathogenic point mutations in the human mitochondrial ND6 subunit are marked by arrows. Sequence sources and their Swiss-Prot accession numbers are (from top to bottom): *P. denitrificans* [P29922] (*16*), *E. coli* K-12 [P33605] (*54*), *Thermus thermophilus* HB-8 [Q56225] (*26*), yeast *Yarrowia lipolytica* [Q9B6E9] (*55*), *Xenopus laevis* [P03927] (*56*), chicken *Gallus gallus* [P18941] (*57*), and *Homo sapiens* [P03923] (*58*).

significantly greater than the ratio for the ISO vesicles. This result, in good agreement with the topological data obtained with anti-MBP serum, indicates that the N-terminus of the MBP-fused Nqo10 subunit is orientated toward the periplasmic phase. Similarly, mutants S114C and R142C were preferentially labeled in the RSO vesicles, implying that S114 and R142 face the periplasmic phase. In contrast, mutants N25C and G84C were labeled to a greater extent in the ISO vesicles, suggesting that N25 and G84 are exposed to the cytoplasmic space. Mutants H168C and W182C also gave rise to the values in favor of the cytoplasmic orientation. This latter result agrees well with that of immunochemical studies using anti-Nqo10c antibodies, and signifies that the C-terminal region of the Nqo10 subunit is directed to the cytoplasmic space. Unexpectedly, the results from labeling of mutants A49C and E50C were ambiguous, precluding definitive conclusion as to the sidedness of these cysteine residues. It could be that this area may be poorly accessible to a large reagent such as AIAS. On the basis of available data, a topological model for the *Paracoccus* Nqo10 was constructed as depicted in Figure 8.

DISCUSSION

To date, very little information is available for the membrane domain of NDH-1/complex I. It is obviously important to understand the structure and functional role of this segment to elucidate the overall mechanism of the entire enzyme complex. We have previously characterized the Nqo7 subunit (*20*) and the Nqo11 subunit (*21*) of *Paracoccus* NDH-1 and, in the present study, explored the Nqo10 subunit. By using the secretable MBP fusion system, the *Paracoccus* Nqo10 subunit could be natively expressed as a fusion protein in *E. coli* membranes. The proper orientation of the expressed protein in the *E. coli* membranes was deduced from the location of the MBP moiety and the C-terminus. With the aid of oppositely oriented membrane vesicles expressing the Nqo10 subunit together with the cysteine-scanning method, we were able to determine the membrane topology of this subunit. Our topological model proposed for the *Paracoccus* Nqo10 subunit has five transmembrane spans (TMs), which agrees with the five stretches of hydrophobic residues originally revealed by the hydropathy profile. Our model also indicates that the N- and C-terminal regions face the periplasmic and the cytoplasmic side, respectively. These topological data were compared with predictions offered by a variety of computer programs developed for analysis of transmembrane regions and orientation, and some representative results are shown in Figure 9. All analyses [TMHMM (*34*), HMMTOP (*35*), MEMSAT (*36*), TopPred2 (*37*), TMpred (*38*), and PHD (*39*)] predicted five transmembrane segments with the N-terminus on the outside (periplasmic side). There were slight discrepancies among the algorithms with regard to the position of the five transmembrane segments. Therefore, the actual boundary of each segment must be determined experimentally.

The Nqo10/ND6 subunit is one of the less phylogenetically conserved NDH-1/complex I subunits (*46*). The primary structure of the N-terminal half which accommodates the first three TMs is somewhat better conserved than that of the C-terminal half. Figure 10 shows the amino acid sequence alignment of the region encompassing the three TMs from various organisms including mammals, fungi, and bacteria. There are only four residues well conserved in this region, all in the TM3 (Y60, G62, V66, and F68 in *Paracoccus* numbering). Among them, Y60 may be of particular interest because of the capability of participating in protonation and thus its potential involvement in proton translocation. According to the proposed topology of the *Paracoccus* Nqo10 subunit, Y60 is located in the middle of TM3. In addition, this residue is almost perfectly conserved among all homologues of Nqo10 currently available in sequence databases. Whether or not this tyrosine residue actually participates in proton translocation of NDH-1 remains to be seen.

Despite the poor conservation of primary structure among species, the gene encoding Nqo10/ND6 has recently been identified as a "hot spot" for pathogenic point mutations in mitochondrial DNA (*22*). Nine mutations leading to eight amino acid changes in seven different positions of this subunit have been found so far to be associated with human diseases. Functional defects of complex I have been reported in some of these mutations (*47*−*50*). Examination of the TMs predicted in our proposed Nqo10 model reveals that all of the mutations reported for the human ND6 gene occur within or near the hydrophobic stretch containing the TM2 and TM3 (Figure 8). It is probably unlikely that a single amino acid substitution causes a drastic change in the structure of Nqo10/ND6 leading to a failure in assembly of the entire complex (*22*). Instead, it can be speculated that mutations on TM2 or TM3 may influence the packing of these putative membrane spanning helices. Consequences of mutations on the function of the human enzyme complex could be tested using the bacterial system. One such attempt was made by Finel's group (*51*) in which site-directed mutagenesis was conducted on the Nqo8/ND1 subunit in the *Paracoccus* NDH-1 targeting the residue that mimics the human mitochondria mutation ND1/3460 and several highly conserved amino acids in its immediate surroundings. The results suggested that the Nqo8/ND1 subunit plays an important role in the binding and reduction of Q. It is anticipated that site-directed mutation studies on the *Paracoccus* Nqo10 subunit involving the residues related to human diseases as well as conserved amino acids in the TM2 and TM3 regions should help to clarify the possible role of this subunit on the activity of NDH-1 and on the structural organization of the membrane segment of the enzyme.

ACKNOWLEDGMENT

We thank Dr. Peter Sims for critical reading of the manuscript and Drs. Byoung Boo Seo, Eiko Nakamaru-Ogiso, and M. Isabel Velázquez-López for helpful discussion.

REFERENCES

1. Stouthamer, A. H. (1992) Metabolic pathways in *Paracoccus denitrificans* and closely related bacteria in relation to the phylogeny of prokaryotes. *Antonie Van Leeuwenhoek 61*, 1−33.
2. Yagi, T., Yano, T., Di Bernardo, S., and Matsuno-Yagi, A. (1998) Procaryotic complex I (NDH-1), an overview. *Biochim. Biophys. Acta 1364*, 125−133.
3. Carroll, J., Shannon, R. J., Fearnley, I. M., Walker, J. E., and Hirst, J. (2002) Definition of the nuclear encoded protein composition of bovine heart mitochondrial complex I: Identification of two new subunits. *J. Biol. Chem. 277*, 50311−50317.
4. Yagi, T. (1993) The bacterial energy-transducing NADH-quinone oxidoreductases. *Biochim. Biophys. Acta 1141*, 1−17.
5. Yagi, T., Yano, T., and Matsuno-Yagi, A. (1993) Characteristics of the energy-transducing NADH-quinone oxidoreductase of *Paracoccus denitrificans* as revealed by biochemical, biophysical, and molecular biological approaches. *J. Bioenerg. Biomembr. 25*, 339−345.
6. Guénebaut, V., Vincentelli, R., Mills, D., Weiss, H., and Leonard, K. R. (1997) Three-dimensional structure of NADH-dehydrogenase from *Neurospora crassa* by electron microscopy and conical tilt reconstruction. *J. Mol. Biol. 265*, 409−418.
7. Guénebaut, V., Schlitt, A., Weiss, H., Leonard, K., and Friedrich, T. (1998) Consistent structure between bacterial and mitochondrial NADH: ubiquinone oxidoreductase (complex I). *J. Mol. Biol. 276*, 105−112.
8. Grigorieff, N. (1998) Three-dimensional structure of bovine NADH: Ubiquinone oxidoreductase (Complex I) at 22 Å in ice. *J. Mol. Biol. 277*, 1033−1046.
9. Takano, S., Yano, T., and Yagi, T. (1996) Structural studies of the proton-translocating NADH-quinone oxidoreductase (NDH-1) of *Paracoccus denitrificans*: Identity, property, and stoichiometry of the peripheral subunits. *Biochemistry 35*, 9120−9127.
10. Yano, T., and Yagi, T. (1999) H^+-translocating NADH-quinone-oxidoreductase (NDH-1) of *Paracoccus denitrificans*: Studies on topology and stoichiometry of the peripheral subunits. *J. Biol. Chem. 274*, 28606−28611.
11. Schuler, F., Yano, T., Di Bernardo, S., Yagi, T., Yankovskaya, V., Singer, T. P., and Casida, J. E. (1999) NADH-quinone oxidoreductase: PSST subunit couples electron transfer from iron−sulfur cluster N2 to quinone. *Proc. Natl. Acad. Sci. U.S.A. 96*, 4149−4153.
12. Yano, T., Magnitsky, S., Sled, V. D., Ohnishi, T., and Yagi, T. (1999) Characterization of the putative 2x[4Fe-4S] binding NQO9 subunit of the proton-translocating NADH-quinone oxidoreductase (NDH-1) of *Paracoccus denitrificans*: Expression, reconstitution, and EPR characterization. *J. Biol. Chem. 274*, 28598−28605.
13. Yano, T., and Yagi, T. (1999) H^+-translocating NADH-quinone oxidoreductase (NDH-1) of *Paracoccus denitrificans*: Studies on topology and stoichiometry of the peripheral subunits. *J. Biol. Chem. 274*, 28606−28611.
14. Di Bernardo, S., and Yagi, T. (2001) Direct interaction between a membrane domain subunit and a connector subunit in the H^+-translocating NADH-quinone oxidoreductase. *FEBS Lett. 508*, 385−388.
15. Xu, X., Matsuno-Yagi, A., and Yagi, T. (1992) Gene cluster of the energy-transducing NADH-quinone oxidoreductase of *Paracoccus denitrificans*: characterization of four structural gene products. *Biochemistry 31*, 6925−6932.
16. Xu, X., Matsuno-Yagi, A., and Yagi, T. (1993) DNA sequencing of the seven remaining structural genes of the gene cluster encoding the energy-transducing NADH-quinone oxidoreductase of *Paracoccus denitrificans*. *Biochemistry 32*, 968−981.
17. Chomyn, A., Mariottini, P., Cleeter, M. W. J., Ragan, C. I., Matsuno-Yagi, A., Hatefi, Y., Doolittle, R. F., and Attardi, G. (1985) Six Unidentified Reading Frames of Human Mitochondrial DNA Encode Components of the Respiratory-Chain NADH Dehydrogenase. *Nature 314*, 591−597.
18. Chomyn, A., Cleeter, M. W. J., Ragan, C. I., Riley, M., Doolittle, R. F., and Attardi, G. (1986) URF6, last unidentified reading frame of human mtDNA, codes for an NADH dehydrogenase subunit. *Science 234*, 614−618.
19. Yagi, T., Seo, B. B., Di Bernardo, S., Nakamaru-Ogiso, E., Kao, M.-C., and Matsuno-Yagi, A. (2001) NADH Dehydrogenases: From basic science to biomedicine. *J. Bioenerg. Biomembr. 33*, 233−242.
20. Di Bernardo, S., Yano, T., and Yagi, T. (2000) Exploring the Membrane Domain of the Reduced Nicotinamide Adenine Dinucleotide-Quinone Oxidoreductase of *Paracoccus denitrificans*: Characterization of the NQO7 Subunit. *Biochemistry 39*, 9411−9418.
21. Kao, M.-C., Di Bernardo, S., Matsuno-Yagi, A., and Yagi, T. (2002) Characterization of the Membrane Domain Nqo11 Subunit of the Proton-Translocating NADH-Quinone Oxidoreductase of *Paracoccus denitrificans*. *Biochemistry 41*, 4377−4384.

22. Chinnery, P. F., Brown, D. T., Andrews, R. M., Singh-Kler, R., Riordan-Eva, P., Lindley, J., Applegarth, D. A., Turnbull, D. M., and Howell, N. (2001) The mitochondrial ND6 gene is a hot spot for mutations that cause Leber's hereditary optic neuropathy. *Brain 124*, 209−218.
23. Han, A.-L., Yagi, T., and Hatefi, Y. (1989) Studies on the Structure of NADH: Ubiquinone Oxidoreductase Complex: Topography of the Subunits of the Iron−Sulfur Protein Component. *Arch. Biochem. Biophys. 275*, 166−173.
24. Han, A.-L., Yagi, T., and Hatefi, Y. (1988) Studies on the Structure of NADH: Ubiquinone Oxidoreductase Complex: Topography of the Subunits of the Iron−Sulfur Flavoprotein Component. *Arch. Biochem. Biophys. 267*, 490−496.
25. Hekman, C., and Hatefi, Y. (1991) The F_o subunits of bovine mitochondrial ATP synthase complex: Purification, antibody production, and interspecies cross- immunoreactivity. *Arch. Biochem. Biophys. 284*, 90−97.
26. Yano, T., Chu, S. S., Sled, V. D., Ohnishi, T., and Yagi, T. (1997) The proton-translocating NADH-quinone oxidoreductase (NDH-1) of thermophilic bacterium *Thermus thermophilus* HB-8: Complete DNA sequence of the gene cluster and thermostable properties of the expressed NQO2 subunit. *J. Biol. Chem. 272*, 4201−4211.
27. Kaback, H. R. (1971) Bacterial membranes. *Methods Enzymol. 22*, 99−120.
28. Kim, Y. J., Rajapandi, T., and Oliver, D. (1994) SecA protein is exposed to the periplasmic surface of the *E. coli* inner membrane in its active state. *Cell 78*, 845−853.
29. Holloway, P. W. (1973) A simple procedure for removal of Triton X-100 from protein samples. *Anal. Biochem. 53*, 304−308.
30. Lakowicz, J. R. (1983) *Principles of Fluorescence Spectroscopy*, Plenum Press, New York.
31. Lentz, B. R., Barenholz, Y., and Thompson, T. E. (1976) Fluorescence depolarization studies of phase transitions and fluidity in phospholipid bilayers I. Single component phosphatidylcholine liposomes. *Biochemistry 15*, 4521−4528.
32. Devereux, J., Haeberli, P., and Smithies, O. (1984) A comprehensive set of sequence analysis programs for the VAX. *Nucleic Acids Res. 12*, 387−395.
33. Altschul, S. F., Madden, T. L., Schaffer, A. A., Zhang, J., Zhang, Z., Miller, W., and Lipman, D. J. (1997) Gapped BLAST and PSI−BLAST: a new generation of protein database search programs. *Nucleic Acids Res. 25*, 3389−3402.
34. Krogh, A., Larsson, B., Von Heijne, G., and Sonnhammer, E. L. L. (2001) Predicting trnasmembrane protein topology with a hidden Markov model: Application to complete genomes. *J. Mol. Biol. 305*, 567−580.
35. Tusnády, G. E., and Simon, I. (2001) The HMMTOP transmembrane topology prediction server. *Bioinformatics 17*, 849−850.
36. Jones, D. T., Taylor, W. R., and Thornton, J. M. (1994) A model recognition approach to the prediction of all-helical membrane protein structure and topology. *Biochemistry 33*, 3038−3049.
37. Claros, M. G., and Von Heijne, G. (1994) TopPred II: An improved software for membrane protein structure predictions. *Comput. Appl. Biosci. 10*, 685−686.
38. Hofmann, K., and Stoffel, W. (1993) TMbase- A database of membrane spanning proteins segments. *Biol. Chem. Hoppe Seyler 374*, 166.
39. Rost, B., Fariselli, P., and Casadio, R. (1996) Topology prediction for helical transmembrane proteins at 86% accuracy. *Protein Sci. 5*, 1704−1718.
40. Laemmli, U. K. (1970) Cleavage of structural proteins during the assembly of the head of bacteriophage T4. *Nature 227*, 680−685.
41. Yagi, T., and Hatefi, Y. (1988) Identification of the DCCD-Binding Subunit of NADH−Ubiquinone Oxidoreductase (Complex I). *J. Biol. Chem. 263*, 16150−16155.
42. Anderson, D. J., and Blobel, G. (1983) Immunoprecipitation of proteins from cell-free translation. *Methods Enzymol. 96*, 111−120.
43. Bentlage, H. A. C. M., Janssen, A. J. M., Chomyn, A., Attardi, G., Walker, J. E., Schagger, H., Sengers, R. C. A., and Trijbels, F. J. M. (1995) Multiple deficiencies of mitochondrial DNA- and nuclear- encoded subunits of respiratory NADH dehydrogenase detected with peptide- and subunit-specific antibodies in mitochondrial myopathies. *Biochim. Biophys. Acta 1234*, 63−73.
44. Miller, K. W., Konen, P. L., Olson, J., and Ratanavanich, K. M. (1993) Membrane protein topology determination by proteolysis of maltose binding protein fusions. *Anal. Biochem. 215*, 118−128.
45. Miller, K. W., and Jewell, J. E. (1995) Identification of a topolog control domain in the tetracycline resistance protein. *Arch. Biochem. Biophys. 322*, 445−452.
46. Fearnley, I. M., and Walker, J. E. (1992) Conservation of sequences of subunits of mitochondrial complex I and their relationships with other proteins. *Biochim. Biophys. Acta 1140*, 105−134.
47. Oostra, R. J., Van Galen, M. J. M., Bolhuis, P. A., Bleeker-Wagemakers, E. M., and Van den Bogert, C. (1995) The mitochondrial DNA mutation ND6*14484C associated with Leber hereditary optic neuropathy, leads to deficiency of Complex I of the respiratory chain, *Biochem. Biophys. Res. Commun. 215*, 1001−1005.
48. Jun, A. S., Trounce, I. A., Brown, M. D., Shoffner, J. M., and Wallace, D. C. (1996) Use of transmitochondrial cybrids to assign a complex I defect to the mitochondrial DNA-encoded NADH dehydrogenase subunit 6 gene mutation at nucleotide pair 14459 that causes Leber hereditary optic neuropathy and dystonia. *Mol. Cell. Biol. 16*, 771−777.
49. Carelli, V., Ghelli, A., Bucchi, L., Montagna, P., De Negri, A., Leuzzi, V., Carducci, C., Lenaz, G., Lugaresi, E., and Degli Esposti, M. (1999) Biochemical features of mtDNA 14484 (ND6/M64V) point mutation associated with Leber's hereditary optic neuropathy. *Ann. Neurol. 45*, 320−328.
50. Ravn, K., Wibrand, F., Hansen, F. J., Horn, N., Rosenberg, T., and Schwartz, M. (2001) An mtDNA mutation, 14453G → A, in the NADH dehydrogenase subunit 6 associated with severe MELAS syndrome. *Eur. J. Hum. Genet. 9*, 805−809.
51. Zickermann, V., Barquera, B., Wikström, M., and Finel, M. (1998) Analysis of the pathogenic human mitochondrial mutation ND1/3460, and mutations of strictly conserved residues in its vicinity, using the bacterium *Paracoccus denitrificans*. *Biochemistry 37*, 11792−11796.
52. Beitz, E. (2000) T(E)Xtopo: shaded membrane protein topology plots in LAT(E)X2epsilon. *Bioinformatics 16*, 1050−1051.
53. Kyte, J., and Doolittle, R. F. (1982) A simple method for displaying the hydropathic character of a protein. *J. Mol. Biol. 157*, 105−132.
54. Blattner, F. R., Plunkett, G., III, Bloch, C. A., Perna, N. T., Burland, V., Riley, M., Collado-Vides, J., Glasner, J. D., Rode, C. K., Mayhew, G. F., Gregor, J., Davis, N. W., Kirkpatrick, H. A., Goeden, M. A., Rose, D. J., Mau, B., and Shao, Y. (1997) The Complete Genome Sequence of *Escherichia coli* K-12. *Science 277*, 1453−1474.
55. Kerscher, S., Durstewitz, G., Casaregola, S., Gaillardin, C., and Brandt, U. (2001) The complete mitochondrial genome of *Yarrowia lipolytica, Comp. Funct. Genomonics 2*, 80−90.
56. Roe, B. A., Ma, D. P., Wilson, R. K., and Wong, J. F. (1985) The complete nucleotide sequence of the *Xenopus laevis* mitochondrial genome. *J. Biol. Chem. 260*, 9759−9774.
57. Desjardins, P., and Morais, R. (1990) Sequence and gene organization of the chicken mitochondrial genome. A novel gene order in higher vertebrates. *J. Mol. Biol. 212*, 599−634.
58. Anderson, S., Bankier, A. T., Barrell, B. G., de Bruijn, M. H., Coulson, A. R., Drouin, J., Eperon, I. C., Nierlich, D. P., Roe, B. A., Sanger, F., Schreier, P. H., Smith, A. J., Staden, R., and Young, I. G. (1981) Sequence and organization of the human mitochondrial genome. *Nature 290*, 457−465.

BI034166Z